NOTES AND CORRESPONDENCE

Application of a Third-Order Upwind Scheme in the NCAR Ocean Model*

WILLIAM R. HOLLAND, JULIANNA C. CHOW, AND FRANK O. BRYAN

National Center for Atmospheric Research,+ Boulder, Colorado

29 April 1997 and 22 September 1997

ABSTRACT

The National Center for Atmospheric Research (NCAR) Ocean Model has been developed for use in NCAR's Climate System Modeling project, a comprehensive development of a coupled ocean–atmosphere–sea ice–land surface model of the global climate system. As part of this development, new parameterizations of diffusive mixing by unresolved processes have been implemented for the tracer equations in the model. Because the strength of the mixing depends upon the density structure under these parameterizations, it is possible that local explicit mixing may be quite small in selected locations, in contrast to the constant diffusivity model generally used. When a spatially centered advection scheme is used in the standard model configuration, local overshooting of tracer values occurs, leading to unphysical maxima and minima in the fields. While the immediate problem is a local Gibbs's phenomenon, there is the possibility that such local tracer anomalies might propagate by advection and diffusion far from the source, causing inaccuracies in the tracer fields globally.

Because of these issues, a third-order upwind scheme was implemented for the advection of tracers. Numerical experiments show that this scheme is computationally efficient compared to alternatives (such as the flux-corrected transport scheme) and that it works well with other aspects of the model, such as acceleration (important for spinup efficiency) and the new mixing parameterizations. The scheme mimimizes overshooting effects while keeping the dissipative aspect of the advective operator reasonably small. The net effect is to produce solutions in which the large-scale fields are affected very little while local extrema are nearly (but not completely) removed, leading to physically much more realistic tracer patterns.

1. Introduction

The physical parameterizations and numerical choices in making use of the Geophysical Fluid Dynamics Laboratory (GFDL) ocean modeling code (Cox 1984) are continually evolving. The reason for this is that there is a need for better and more comprehensive parameterizations of subgrid-scale ocean physical processes in a variety of parameter ranges (especially resolution) as ocean modelers seek high quality solutions relative to observations.

Advective schemes in ocean models and in computational fluid mechanics problems in general have a vast literature regarding space and time discretization issues. In the original GFDL code, a simple centered-in-time, centered-in-space (CTCS) advective scheme was chosen using a finite volumes formulation, with the tracer values at the edge of tracer cells set to averages of the adjacent cell tracer values (Bryan 1966, 1969). This choice allowed the conservation of mass (volume in the Boussinesq approximation), tracer concentration, and tracer variance in the fluid interior.

To run the model, however, diffusive terms were added to the tracer advection equation for both physical and numerical reasons, that is, both to represent subgrid-scale mixing processes and to allow reasonably smooth fields at or near the grid scale. Laplacian diffusive terms in both the horizontal and vertical directions covered up many difficulties of the advection scheme, as long as the coefficients of diffusion were ''large enough.''

During development of the National Center for Atmospheric Research (NCAR) version of the GFDL model (NCOM) as the ocean component of the global Climate System Model (CSM), two new mixing parameterizations were introduced. The first is due to Gent and McWilliams (1990), hereafter GM90, and is based upon a thickness mixing hypothesis that leads to bolus velocity terms in the tracer equation. This bolus advection is used in concert with a diffusive isopycnal mixing process as in Redi (1982). These terms produce tracer fluxes and flux divergences in all three dimensions. The second parameterization (Large et al. 1994, hereafter called the KPP scheme) handles vertical mixing in the

* An electronic supplement to this article may be found on the CD-ROM accompanying this issue or at http://www.ametsoc.org/AMS.

+ The National Center for Atmospheric Research is sponsored by the National Science Foundation.

Corresponding author address: Dr. William R. Holland, NCAR/CGD, P.O. Box 3000, Boulder, CO 80307-3000.
E-mail: holland@ucar.edu

upper ocean boundary layer but also includes a dependence upon the vertical density gradient and vertical shear of the horizontal velocity that can enhance deep mixing in convectively unstable regions. The model can then be run without convective adjustment but does include a background vertical diffusion.

As these mixing parameterizations were developed and tested, it was found that local extrema in the tracer fields had a much greater tendency to develop than in the standard horizontal–vertical diffusion schemes, especially in regions near overflows like the Mediterranean outflow from the Strait of Gibralter into the North Atlantic and the overflow in the Denmark Strait of the model. The amplitude of the unphysical extrema became larger as the horizontal resolution of the model was changed from 3° to 2° to 1° grid size. It became clear that this was a classic problem with centered spatial differencing in the presence of quite small local explicit mixing. The problem is exacerbated by the fact that the isopycnal mixing in NCOM tapers to zero in the presence of steep isopycnal slopes (which in overflow regions may be topographically defined). See Large et al. (1997) for a discussion of these tapering issues. As pointed out by Gerdes et al. (1991), the bottom topography can interact with vertical mixing to cause local extrema. The local Peclet number can also get substantially larger in localities with strong vertical velocities such as overflow locations.

The problem of central differencing has been addressed in the context of the GFDL model before (Gerdes et al. 1991; Hecht et al. 1995; Farrow and Stevens 1995). The basic idea is to allow the numerical algorithm for advection to have an upstream-weighted form with a consequent loss of the variance preserving character of the original Bryan–Cox form. Leonard (1979) developed the basis for a whole host of such schemes that are accurate to third order spatially. Our scheme is a variant of his Quadratic Upstream Interpolation for Convective Kinematics (QUICK) scheme (Leonard 1979) and, although developed independently for a different parameter range (coarse resolution vs fine resolution), is identical to that of Farrow and Stevens (1995, hereafter FS95) as far as the spatial scheme is concerned. We chose, however, to stay with the time-stepping scheme already present in the GFDL model rather than the more complex predictor–corrector scheme of FS95.

Below we present the advection scheme and model results to show that such a scheme is useful and even necessary in global, noneddy-resolving models that include more complex mixing schemes like those of GM90 and KPP. Using a third-order upwind scheme makes possible high quality solutions with a minimum of smoothing of the large-scale fields.

2. The finite difference advection scheme

The conservation equation for some tracer, S, may be written in flux form as

$$\frac{\partial S}{\partial t} = -[(uS)_x + (vS)_y + (wS)_z] + DIF. \quad (1)$$

This equation is the mathematical statement that the tracer S (e.g., temperature and salinity) is advected by the fluid motion in a conservative fashion (no net gain or lost following fluid particles), except due to diffusive effects. The right-hand-side term *DIF* in (1) simply represents the sum of all the diffusive effects, notably isopycnal diffusion, diapycnal diffusion, and KPP mixing effects. The GM90 parameterization of subgrid-scale mixing effects that lead to an eddy-induced velocity field are included in the advective velocity field (u, v, w) in the directions x (zonal), y (meridional), and z (upward).

Let us focus first upon the spatial discretization of the advective term on the right-hand side of (1). We shall return to issues associated with time discretization later. Here we follow the notation of FS95. For simplicity in presentation we show here only the zonal part of the advection operator. The meridional and vertical terms have exactly comparable forms. Note, however, that the vertical grid is often highly variable in the vertical coordinate; that is, the Δz's can vary by a factor of 10 to 20 times over the depth of the ocean, compared to order of two times in Δx or Δy. This will affect the details and interpretation of the upwind operator in an important way. Note also that the upwinding is done independently in each coordinate direction.

As shown by FS95, the form for the third-order upwind advective operator depends on the sign of the velocities u_l and u_r on the left- and right-hand sides of a tracer cell. With a variable grid (Δx varying with x), the operator becomes a little complicated but can be developed from a straightforward Taylor's series expansion, given the location of the centers of the tracer cells and the locations of the cell boundaries. The contribution to $\partial S/\partial t$ due to zonal advective fluxes can be written (subscripts r and l for right and left cell faces, respectively, and subscripts p and m for plus [$u \geq 0$] and minus [$u < 0$] flow directions, respectively)

$$\frac{\partial S}{\partial t} = -\frac{u_r}{\Delta x_i}\left[\frac{\Delta x_{i+1} S_i + \Delta x_i S_{i+1}}{\Delta x_{i+1} + \Delta x_i} - \frac{1}{8}\mathrm{CURV}_r\right] + \frac{u_l}{\Delta x_i}\left[\frac{\Delta x_i S_{i-1} + \Delta x_{i-1} S_i}{\Delta x_{i-1} + \Delta x_i} - \frac{1}{8}\mathrm{CURV}_l\right], \quad (2)$$

where, if $u_l > 0$, CURV_l becomes

$$\mathrm{CURV}_{lp} = \frac{8\Delta x_{i-1}\Delta x_i}{\Delta x_{i-2} + 2\Delta x_{i-1} + \Delta x_i} \times \left(\frac{S_i - S_{i-1}}{\Delta x_{i-1} + \Delta x_i} - \frac{S_{i-1} - S_{i-2}}{\Delta x_{i-2} + \Delta x_{i-1}}\right) \quad (3)$$

and, if $u_l < 0$, CURV_l becomes

$$\mathrm{CURV}_{lm} = \frac{8\Delta x_{i-1}\Delta x_i}{\Delta x_{i-1} + 2\Delta x_i + \Delta x_{i+1}} \times \left(\frac{S_{i+1} - S_i}{\Delta x_i + \Delta x_{i+1}} - \frac{S_i - S_{i-1}}{\Delta x_{i-1} + \Delta x_i}\right). \quad (4)$$

Also, if $u_r > 0$, CURV_r becomes

$$\mathrm{CURV}_{rp} = \frac{8\Delta x_i\Delta x_{i+1}}{\Delta x_{i-1} + 2\Delta x_i + \Delta x_{i+1}} \times \left(\frac{S_{i+1} - S_i}{\Delta x_i + \Delta x_{i+1}} - \frac{S_i - S_{i-1}}{\Delta x_{i-1} + \Delta x_i}\right) \quad (5)$$

and if $u_r < 0$, CURV_r becomes

$$\mathrm{CURV}_{rm} = \frac{8\Delta x_i\Delta x_{i+1}}{\Delta x_i + 2\Delta x_{i+1} + \Delta x_{i+2}} \times \left(\frac{S_{i+2} - S_{i+1}}{\Delta x_{i+1} + \Delta x_{i+2}} - \frac{S_{i+1} - S_i}{\Delta x_i + \Delta x_{i+1}}\right). \quad (6)$$

In order to write a single equation for (2) and at the same time identify the diffusive component of the upwind scheme, it is useful to combine the several CURV terms as follows (subscripts *a* and *d* stand for average and difference quantities).

Let $\mathrm{CURV}_{ra} = (\mathrm{CURV}_{rp} + \mathrm{CURV}_{rm})/2$ and $\mathrm{CURV}_{rd} = (\mathrm{CURV}_{rp} - \mathrm{CURV}_{rm})$. Also $\mathrm{CURV}_{la} = (\mathrm{CURV}_{lp} + \mathrm{CURV}_{lm})/2$ and $\mathrm{CURV}_{ld} = (\mathrm{CURV}_{lp} - \mathrm{CURV}_{lm})$. Then Eq. (2) can be written

$$\frac{\partial S}{\partial t} = -\frac{u_r}{\Delta x_i}\left[\frac{\Delta x_{i+1}S_i + \Delta x_i S_{i+1}}{\Delta x_{i+1} + \Delta x_i} - \frac{1}{8}\mathrm{CURV}_{ra}\right] + \frac{u_l}{\Delta x_i}\left[\frac{\Delta x_i S_{i-1} + \Delta x_{i-1}S_i}{\Delta x_{i-1} + \Delta x_i} - \frac{1}{8}\mathrm{CURV}_{la}\right] + \frac{|u_r|}{16\Delta x_i}\mathrm{CURV}_{rd} - \frac{|u_l|}{16\Delta x_i}\mathrm{CURV}_{ld}. \quad (7)$$

For a uniform spatial discretization, the above equations reduce to

$$\mathrm{CURV}_{lp} = S_i - 2S_{i-1} + S_{i-2}$$

$$\mathrm{CURV}_{lm} = S_{i+1} - 2S_i + S_{i-1}, \quad (8)$$

$$\mathrm{CURV}_{rp} = S_{i+1} - 2S_i + S_{i-1}$$

$$\mathrm{CURV}_{rm} = S_{i+2} - 2S_{i+1} + S_i, \quad (9)$$

$$\mathrm{CURV}_{la} = \frac{S_{i+1} - S_i - S_{i-1} + S_{i-2}}{2}$$

$$\mathrm{CURV}_{ld} = -S_{i+1} + 3S_i - 3S_{i-1} + S_{i-2}, \quad (10)$$

$$\mathrm{CURV}_{ra} = \frac{S_{i+2} - S_{i+1} - S_i + S_{i-1}}{2}$$

$$\mathrm{CURV}_{rd} = -S_{i+2} + 3S_{i+1} - 3S_i + S_{i-1}. \quad (11)$$

It is readily apparent that for constant Δx,

$$\mathrm{CURV}_{ld} = -\Delta x^3\left(\frac{\partial^3 S}{\partial x^3}\right)_{i-1/2}$$

$$\mathrm{CURV}_{rd} = -\Delta x^3\left(\frac{\partial^3 S}{\partial x^3}\right)_{i+1/2}. \quad (12)$$

It can be verified that with nonconstant Δx, these terms are also equal to the third derivative of S evaluated on the cell interfaces.

The terms in square brackets in (7) are quadratic interpolations of the tracer field S to the respective interfaces. For constant Δx, they reduce to

$$\left[\ \right]_{i+1/2} = \frac{-S_{i+2} + 9S_{i+1} + 9S_i - S_{i-1}}{16}$$

$$\left[\ \right]_{i-1/2} = \frac{-S_{i+1} + 9S_i + 9S_{i-1} - S_{i-2}}{16}. \quad (13)$$

These quantities show that (7) can be written in the form

$$\frac{\partial S}{\partial t} = -\frac{\partial}{\partial x}\left[u\hat{S}\right] - \frac{\partial}{\partial x}\left[A_{bh}\frac{\partial^3 S}{\partial x^3}\right], \quad (14)$$

where $A_{bh} = |u|\Delta^3/16$ and $\hat{S}$ is equal to the interpolated tracer value at the interfaces of the grid cells, that is, the terms in the square brackets in (7). Here $\Delta^3 = \Delta x_i\Delta x_{i+1}(\Delta x_i + \Delta x_{i+1})/2$ for the right-hand cell face. Here A_{bh} is a spatially dependent biharmonic diffusivity and $\hat{S}$ is a quadratic interpolation of S to the respective interfaces of tracer cells. The CURV terms in $\hat{S}$ are the adjustments for curvature in S. We shall call this scheme UPW3 (for third-order upwind).

Regarding the temporal discretization of (14) for leapfrog time stepping, stability considerations suggest the correct choice is to evaluate $\hat{S}$ at the centered time step n and to evaluate the diffusive term in A_{bh} at the lagged time step $n - 1$ (Richtmeyer and Morton 1967). FS95 elected to use a predictor–corrector method. We have examined several choices within the context of model

TABLE 1. Numerical experiments testing the third-order upwind scheme (UPW3) in relation to the standard CTCS scheme and a first-order upwind (donor cell) scheme (DONR). Here, $\hat{S}_c = (S_i + S_{i+1})/2$ and $\hat{S}_u$ is the full UPW3 form in the square brackets of (7). The A_{bh} term is used in UPW3 and the A_{lp} in DONR. The right-hand columns show two locations (outlier 1, a maximum in salinity, is at the Mediterranean outflow and outlier 2, a minimum in temperature, is just south of the Denmark Strait overflow). The values are the extreme values of S (first column) or T (second column), while the values in parentheses are the nearest neighbor (of the six surrounding values) that is closest in value to the extrema. This is a simple measure of how vigorous the overshooting is at that location.

CASE	$\hat{S}$	A_{bh}	A_{lp}	Outlier 1 S(149, 71, 16)	Outlier 2 T(135, 90, 16)
CTCS_c	$\hat{S}_c$	—	—	40.38 (38.68)	−4.68 (−1.87)
CTCS_u	$\hat{S}_u$	—	—	39.64 (38.43)	−4.33 (−1.78)
UPW3	$\hat{S}_u$	$\lvert u\rvert\Delta^3/16$	—	39.47 (38.96)	−2.48 (−1.92)
DONR	$\hat{S}_c$	—	$\lvert u\rvert\Delta/2$	38.31 (38.84)	−1.26 (−1.77)

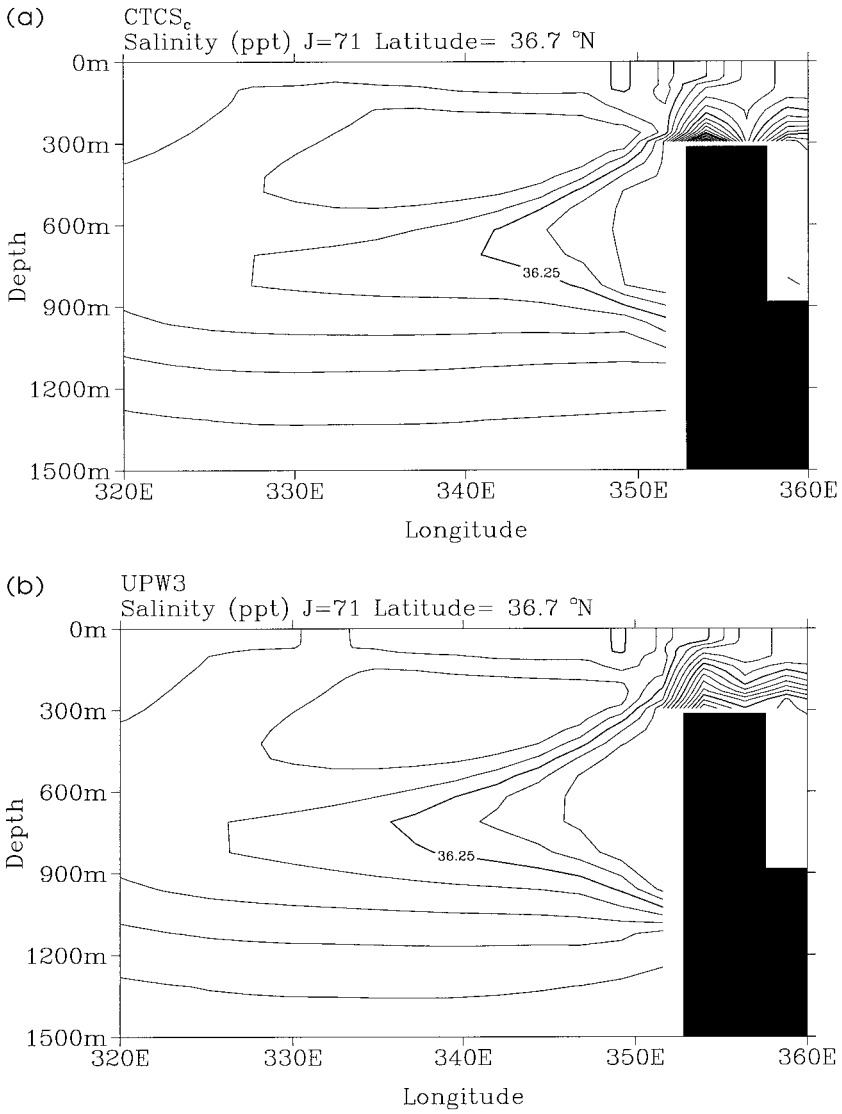

FIG. 1. The salinity field at latitude 36.7°N for the upper 1500 m. The section is taken through the Strait of Gibralter some distance into the Mediterranean Sea. (Upper) Experiment CTCS$_c$; (Lower) experiment UPW3. The contour interval is 0.25‰.

experiments. In the next section we compare numerical model results using the standard CTCS scheme with results using (7) where the biharmonic diffusive term is lagged in time. Also, for completeness, we examine results from a case with donor cell (first-order upwinding) for comparison. For the donor cell scheme (DONR), we have, instead of (14),

$$\frac{\partial S}{\partial t} = -\frac{\partial}{\partial x}\left[u\hat{S}\right] + \frac{\partial}{\partial x}\left[A_{lp}\frac{\partial S}{\partial x}\right], \qquad (15)$$

where $A_{lp} = |u|(\Delta x_i + \Delta x_{i+1})/4$ and $\hat{S}$ is equal to the average tracer value at the interfaces of the grid cells, that is, $(S_{i+1} + S_i)/2$.

3. Tests with a global model and discussion

Several numerical experiments with the global NCAR Ocean GCM used in the CSM coupled model were run in an uncoupled mode to test the effects of alternate advective algorithms. This version of the model has 45 levels in the vertical (12.5 m at the surface) and horizontal resolution of 2.4° in longitude and between 1.2° and 2.3° in latitude (finest at the equator and in high latitudes, coarsest in midlatitudes). Use was made of a very long experiment to equilibrium [the NCOM experiment described in Gent et al. (1998)], which included the first implementation of the third-order upwind scheme. In that case, the biharmonic part on the advection algorithm was not lagged in time. Then sev-

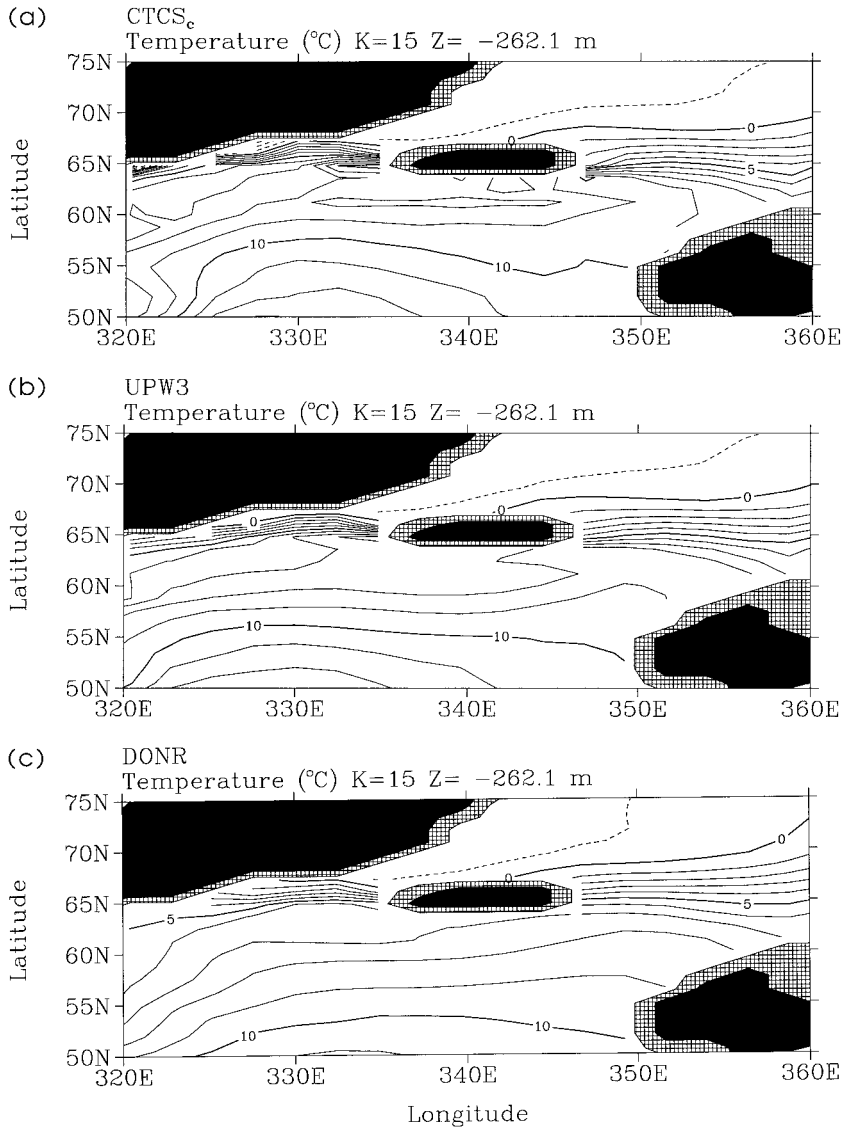

FIG. 2. Horizontal maps (at a depth of 262 m) of the temperature field from three experiments: CTCS$_c$, UPW3, and DONR. The contour interval is 1°C.

eral additional experiments were run, repeating the last 10 yr of the standard case. The experiments were distinguished by having different variants of the advection algorithm as defined below. The instantaneous results were examined and compared at the end of these runs to examine the effects on the fields of temperature and salinity.

Table 1 summarizes the most informative of the numerical experiments run: CTCS (two experiments), UPW3 (one experiment), and DONR (one experiment). The first CTCS experiment consists of the standard Bryan–Cox scheme (CTCS$_c$) and the second scheme uses the full UPW3 version for $\hat{S}$, that is, a full quadratic interpolation but without the diffusive term (CTCS$_u$). The results from this latter experiment suggest that there is some improvement to be gained from the quadratic interpolation itself, even without a diffusive component. The upwind experiment has the $\hat{S}$ form shown in the square brackets of (7) while the A_{bh} term is lagged in time (UPW3). The DONR case, similar to UPW3 but for first-order upwinding, is carried out to examine how useful UPW3 is for preserving gradients, that is, not to cause excessive smoothing. Table 1 also shows a pair of locations at which large outliers in salinity and/or temperature occur with the CTCS scheme. The Mediterranean outflow salinity outlier is an isolated maximum, while the Denmark Strait overflow temperature outlier is an isolated minimum. It may be seen that the outlier value is diminished relative to its immediate neighbors for the UPW3 scheme, relative to CTCS schemes, and the DONR removes the outliers entirely (these points are no longer extrema). In addition to these

experiments, cases were run in which the diffusive terms in UPW3 and DONR were not lagged in time, but there was no hint of instability nor any substantial differences in solutions from the comparable lagged cases.

The reason for the choice of 10 yr was as follows. For a very short run, say a few time steps, the model still contains the imprint of the particular advection operator used to create the initial condition. This might prejudice the comparison of results. A very long run, say many centuries, would allow the models to significantly drift from their basic thermohaline state and perhaps change the conditions that led to the overshooting process in the first place. Again it could be difficult to argue that such comparisons were valid. It was observed, however, that the local outliers in either time and/or space were quickly recovered (within tens of time steps) when the CTCS algorithm was used. However, longer runs showed that there was a slow inexorable drift in the time–space properties over the long timescale that we presume is connected with the removal of the extrema. Since the background diffusive properties are different in the several experiments, this is not surprising. It does give one pause to reflect on the fact that it will be very hard to achieve a detailed and precise recovery of observed oceanic time–space properties given the present state of our knowledge of ocean mixing properties. This is made clear if one looks at the local balances that exist in the heat and salt fluxes that contribute to the flux divergences responsible for the rate of change in the tracer fields. The changes in the advective terms caused by upwinding, for example, are a few percent of the size of the other terms. But these changes diminish local dispersive effects associated with center-in-space differencing, minimizing local unphysical maxima or minima.

East–west/vertical sections in Fig. 1 show the salinity field for one of the strongest outlier locations, that is, the Mediterranean outflow (outlier 1 in Table 1). The large anomalous value in the CTCS case, where the outflowing Mediterranean water mass encounters the North Atlantic waters (producing a large horizontal gradient there), is diminished very substantially in the UPW3 cases, as shown in the right-hand columns of Table 1. The salinity extrema diminish from an excess of 1.7‰ to 0.5‰ between the $CTCS_c$ and UPW3 cases. Note that DONR removes the extremum entirely (adjacent values are larger and smaller than the local value).

Figure 2 shows, however, that the DONR scheme has a rather strong smoothing effect on the large scale, relative to CTCS and UPW3 schemes. The frontal structures are everywhere substantially broader in DONR, while they are mostly preserved when UPW3 is compared with CTCS. The diffusive effects in UPW3 apparently act very locally on those elements that give rise to the overshooting phenomenon.

The motivation for the choice of the QUICK scheme was the promising results in Hecht et al. (1998). The scheme has a much lower computational cost than the alternatives, such as flux corrected transport, and it is found to work well with other aspects of the model such as acceleration (important for spinup efficiency), GM90 (dual velocities), and the KPP scheme. The third-order upwind scheme substantially reduces overshooting effects while keeping the diffusive aspect of the advective operator reasonably small. The net effect is to produce solutions in which the large-scale fields are smoothed only slightly while local extrema are mostly (but not completely) removed, leading to physically much more realistic tracer patterns.

Finally, we reiterate that the scheme works well in the low-resolution (climate) model context. It is not necessary to use the predictor–corrector scheme suggested by FS95 (which is expensive). In fact, in all the experiments, the lag in time (or not) seems to have little or no effect. We could discern no tendency for numerical instabilities and no differences in solutions. We would advocate using the lagged formulation, however, because it may be important in other parameter ranges. Our scheme provides an intermediate choice between CTCS and flux-corrected transport (or DONR) for situations where strict monotonicity is not required. Note that the scheme has been incorporated into Modular Ocean Model 2.2 (Pacanowski 1997).

REFERENCES

Bryan, K., 1966: A scheme for numerical integration of the equations of motion on an irregular grid free of nonlinear instability. *Mon. Wea. Rev.,* **94,** 39–40.

——, 1969: A numerical method for the study of the circulation of the world ocean. *J. Comput. Phys.,* **4,** 347–376.

Cox, M. D., 1984: A primitive equation three-dimensional model of the ocean. Ocean Group Tech. Rep. 1, 141 pp. [Available from Geophysical Fluid Dynamics Laboratory, Princeton University, P.O. Box 308, Princeton, NJ 08542.]

Farrow, D. E., and D. P. Stevens, 1995: A new tracer advection scheme for Bryan and Cox type ocean general circulation models. *J. Phys. Oceanogr.,* **25,** 1731–1741.

Gent, P. R., and J. C. McWilliams, 1990: Isopycnal mixing in ocean circulation models. *J. Phys. Oceanogr.,* **20,** 150–155.

——, F. O. Bryan, G. Danabasoglu, S. C. Doney, W. R. Holland, W. G. Large, and J. C. McWilliams, 1998: The NCAR Climate System Model global ocean component. *J. Climate,* **11**, 1287–1306.

Gerdes, R., C. Köberle, and J. Willebrand, 1991: The influence of numerical advection schemes on the results of ocean general circulation models. *Climate Dyn.,* **5,** 211–226.

Hecht, M. W., W. R. Holland, and P. J. Rasch, 1995: Upwind weighted advection schemes for ocean tracer transport: An evaluation in a passive tracer context. *J. Geophys. Res.,* **100**, 20 763–20 778.

——, F. O. Bryan, and W. R. Holland, 1998: A consideration of tracer advection schemes in a primitive equation ocean model. *J. Geophys. Res.,* **103**, 3301–3322.

Large, W. G., J. C. McWilliams, and S. C. Doney, 1994: Oceanic vertical mixing: A review and a model with a nonlocal boundary layer parameterization. *Rev. Geophys.,* **32,** 363–403.

——, G. Danabasoglu, S. C. Doney, and J. C. McWilliams, 1997: Sensitivity to surface forcing and boundary layer mixing in a global ocean model: Annual-mean climatology. *J. Phys. Oceanogr.,* **27,** 2418–2447.

Leonard, B. P., 1979: A stable and accurate convective modeling procedure based upon quadratic upstream interpolation. *Comput. Methods Appl. Mech. Eng.*, **19,** 59–98.

Pacanowski, R. C., 1996: MOM 2, version 2.0. Documentation user's guide and reference manual. GFDL Ocean Group Tech. Rep. 3.2, 328 pp. [Available from Geophysical Fluid Dynamics Laboratory, Princeton University, P.O. Box 308, Princeton, NJ 08542.]

Redi, M. H., 1982: Oceanic isopycnal mixing by coordinate rotation. *J. Phys. Oceanogr.*, **12,** 1154–1158.

Richtmeyer, R. D., and K. W. Morton, 1967: *Difference Methods for Initial Value Problems.* Wiley, 405 pp.